The evaluation of Sb and SnSb negative electrode materials in full Na-ion cells

Jerry Barker, Fazlil Coowar, Julien Fullenwarth, Laure Monconduit

The evaluation of Sb and SnSb negative electrode materials in full Na-ion cells

Jerry Barker[4], Fazlil Coowar[4], Julien Fullenwarth[1], Laure Monconduit [1,2,3,*]

1- ICGM, Univ. Montpellier, CNRS, Montpellier, France

2- RS2E, CNRS, Amiens, France

3- Alistore-ERI, CNRS FR 3104, Amiens, France

4- Faradion Limited, Innovation Centre, Sheffield, United Kingdom

Abstract

Na-ion batteries (SIB) represent a realistic and important alternative to commercial Li-ion batteries and are expected to play a significant role in future stationary energy storage systems and E-mobility applications. The search for next-generation negative electrode active materials for Na-ion is critically important, especially to replace hard carbon. Based on previous Na half-cell studies which indicated that both Sb and SnSb demonstrated encouraging performance, we have studied the performance of these materials in full Na-ion cells using a mixed phase O3/P2 layered oxide as the positive electrode. By working on the P/N balance, the Na-ion full cells show encouraging performance even at non-optimized cell balances, with an absence of Na plating, and a high cyclability. For the best performing experimental iteration, we predict a specific energy performance close to 183 W h kg^{-1} for a Na-ion cell capacity of 49 Ah based on the data on cell A11017.

Keywords :

Battery, Na-ion, Sb, SnSb, full cells

1. Introduction/Background

The large-scale application of LIBs will need us to account for the limited abundance and associated growing price of the Li resource. Na and Li are chemical neighbours with similar properties and as such Na-ion batteries (SIB) have attracted great attention due to the higher abundance of Na and its significantly lower cost. Historically, the energy density of SIB was expected to be lower due to i) a larger atomic weight and radius of Na than Li and ii) a higher standard potential of Na^+/Na (2.71 V vs. SHE) compared to Li. However today there is increasing realisation that SIB`s can be very competitive and the development of SIB for large-scale energy systems, for example is of significant commercial importance.

With respect to the negative electrode materials for SIBs, it is a great challenge to seek suitable active material with high performance, such as high reversible specific capacity, stable cycling and appropriate operating voltage. In contrast to the case of LIBs, graphite does not intercalate Na^+ when using conventional electrolytes, thus cannot be used directly as the negative electrode in SIB. Hard carbon (HC) has been widely used due to its specific features, highly disordered structure and large interlayer distance. With Na^+ insertion in between/in carbon layers and micropores, HC achieves a reversible specific capacity of around 300 mAh g^{-1}.[1, 2, 3]

Alloying-type negative electrodes, mainly the p-block elements (Ge, Sn, Pb, P, Sb, Bi, etc), usually involve a multiple-electron exchange to form stable alloys and are thus able to lead to very high specific capacities at suitable operation

voltages.[4,5] For example, by offering low redox potential and the ultimate formation of Na_3Sb (660 mAh g^{-1}) antimony is among the most interesting alloying materials for SIB applications.

Although the alloying of these elements with Na causes a strong volume expansion, the cycling in sodium metal half cells have shown very attractive performance.[6] Impressively stable cycling with raw Sb-rich electrodes (70 % wt) was demonstrated, a stable capacity of 580 mAh g^{-1} at a moderate rate was maintained over 160 cycles with a coulombic efficiency over 99 %.[7] The associated mechanism of sodiation was elucidated by in-situ XRD, indicating that Na reacts with crystalline Sb to form intermediate amorphous Na_xSb phases. Operando pair distribution function (PDF) analysis and ex-situ ^{23}Na magic-angle spinning (MAS) solid-state NMR spectroscopy provided significant insight into the alloying mechanism of Sb with Na. The durability of the Sb/Na relies on the elastic softening of the sodiated antimony phases, which enhances the ability of the electrode to absorb and mitigate the strong volume changes upon (de)sodiation.[8]

Methods used to resolve the volume expansion issues include the preparation of Sb nanostructures with the preparation of nanocomposites with Sb nanoparticles embedded in conductive carbon matrices,[9] carbon nanofibers or nanotubes,[10] porous carbon spheres, or graphene layers able to partially accommodate the large volume expansion and improve the conductivity. Despite the interesting achievements of Sb-based composites, their practical applications appear limited by their complex synthesis process, high cost, and low yield.

The design of M–Sb intermetallics, with M being either an electrochemically inactive or an active component, has also been proposed to alleviate volume changes during cycling. When M is electrochemically active vs. Na, it can work as a mutual buffer with Sb to alleviate the volume expansion and simultaneously participate to the global capacity. For example, SnSb, sustains a reversible capacity largely exceeding 525 mAh g^{-1} over more than 125 cycles at a low rate of 55 mA g^{-1}.[11] The reversible sodiation–desodiation reaction of SnSb was also investigated by simultaneous operando Sn and Sb K-edge XAS along with operando ^{119}Sn Mössbauer spectroscopy. The reaction is a two-step reversible conversion and alloying reactions clearly distinct from the reaction of SnSb vs. Li. The key to the enhanced cycle life was proposed to lie in the gradual formation of amorphous, nanoconfined intermediates and correlated to elastic softening of highly sodiated tin and antimony phases, producing a system able to absorb and mitigate the strong volume changes.

Despite their very interesting performances in sodium half cells these two alloying materials, Sb and SnSb, have however been studied poorly in NIB full cells. In this present work we investigate their commercial potential as negative electrodes when matched with a well-defined, mixed-phase O3/P2 layered oxide material $Na_x[Ni/Mn/Mg/Ti]O_2$ positive electrode.

2. Synthesis and Experimental part

SnSb powder synthesis

SnSb material was prepared by ball milling with Sn powder (Aldrich,10 µm, >99%) and Sb powder (Alpha Aeser 99.5% purity, ~325 mesh). A stoichiometric

ratio of both powders was used in a 65mL stainless steel vial with six 10mm diameter balls. Both the jars and the balls are made with hardened stainless steel. An active-milling time of 200 minutes with the 8000M Spex miller was enough to obtain a complete reaction of Sn and Sb. X-ray diffraction (XRD) experiment confirmed that synthesized SnSb (Figure SI-1) crystallizes in the expected R-3m space group with the cell parameters a= 8.629 (2) Å, b= 8.629 (4) Å and c=10.656(2) Å in agreement with those reported in the 00-001-0830 PDF file.

Slurry preparation and electrochemical measurements

For negative electrodes: The electrode was prepared by mixing the active material, Sb (Alpha Aeser 99.5% 325 mesh powder) or as prepared SnSb (70%) with IMERYS C65 carbon black (9%) and carbon fibres -VGCF-S (9%) as conductive additives, and carboxymethylcellulose - CMC (12%) as binder. A quantity of 1.2 ml distilled water was added to the materials and homogeneously mixed by planetary ball-milling for 1 h in 12mL agate vial with 5mm diameter balls. The slurry was tape casted on a copper foil, dried at room temperature for one night and at 100 °C under vacuum for 4 h. The final mass loading of active material on the electrode was between 1.5 and 2 mg cm-².

The positive electrode material was supplied by Faradion and synthesized according to Faradion's specification of a mixed-phase O3/P2 layered oxide.[12]

The electrochemical measurements of the prepared electrodes were first tested vs a Na foil in coin cells assembled in an argon filled glove box. The electrolyte was 1 M $NaPF_6$, in propylene carbonate (PC) as solvent and fluoroethylene

carbonate (FEC) (5%) as additives. Whatman glass fibre filter were used as separator. The half-cell was cycled with a C/6 and C/10 rate. The galvanostatic charge/discharge measurements were carried out at room temperature on Biologic battery testing system.

For the full cell electrochemical tests, the electrolyte comprised a 1M solution of $NaPF_6$ in a solvent mixture of ethylene carbonate, diethyl carbonate and propylene carbonate (with no additives). To accurately establish and assess the electrochemical performance and the useable reversible specific capacity of the Sn and SnSb electrodes various positive to negative active mass balances were used. This experimental approach is summarized in the tables 1 and 2 below.

3. Results

Na Half Cell Electrochemistry

The voltage profile of the first discharge of Sb vs. Na (Figure 1-a) measured at 110 mA/g shows a first insertion of Na along a single long plateau at 0.45 V, while the second discharge and the following ones, show three distinct plateaus at 0.72, 0.55, and 0.50 V. In charge, the first de-sodiation and the following ones show the presence of two plateaus, a first long plateau at 0.80 V and a shorter one at 0.9 V. The associated electrochemical mechanism was elucidated from PDF and NMR which identified two new intermediate species formed electrochemically; a-$Na_{3-x}Sb$ ($x \approx 0.4$ - 0.5), a disordered structure locally similar to crystalline Na_3Sb and a-$Na_{1.7}Sb$, a highly amorphous structure featuring some Sb-Sb bonding.[8]

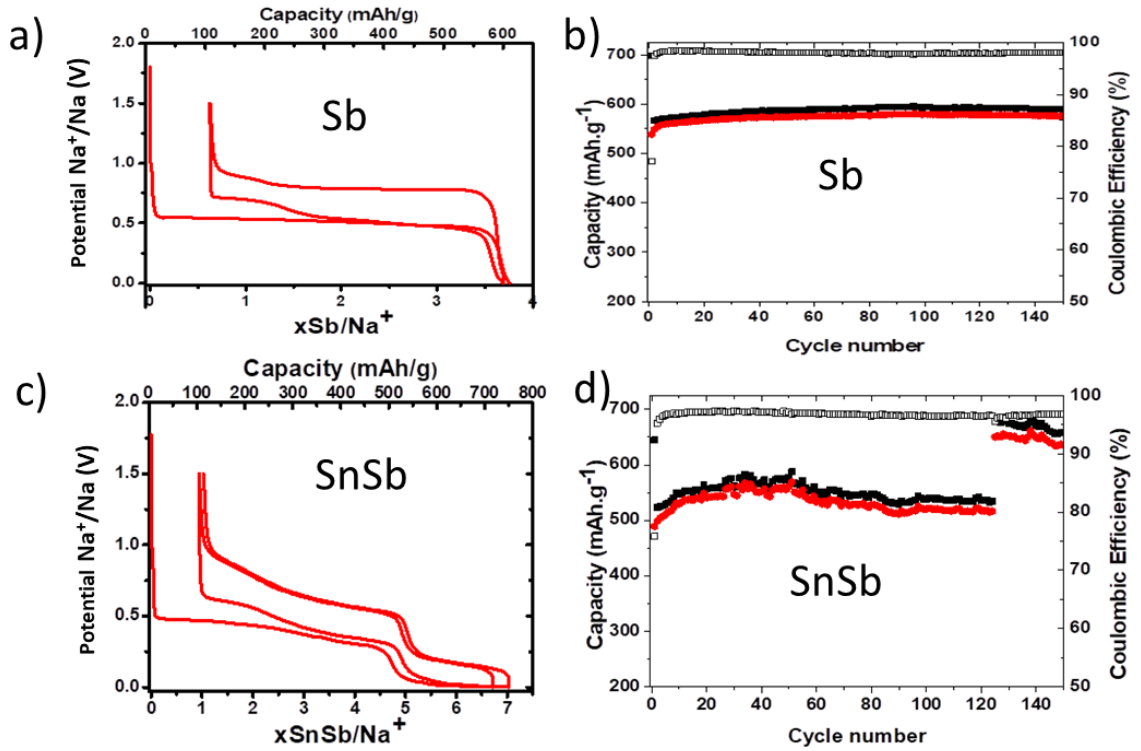

***Figure 1**: Composition-voltage profile (a, c) and capacity retention with cycles (b, d) for Sb/Na (cycled at C/6) and SnSb/Na respectively (cycled at C/10). c) the SnSb/Na Composition-voltage profile is measured in the [1.5-0 V], when the cycling retention has been measured in the [1.5-0.02V] voltage window for the 120 first cycles and measured in the [1.5-0.0V] voltage window in further cycles.*

The profile of the first discharge of SnSb vs. Na measured at 55 mA/g is shown in Figure 1-c, and the capacity retention (measured first in the limited potential window of [1.5-0.02V] and thereafter in the full voltage window of [1.5-0.0V]) in Figure 1-d. About 4.9 Na are reversibly inserted when the lower potential was fixed to 0.02 V, corresponding to a 520 mAh g^{-1} capacity, while 6 Na can be reversibly inserted in the whole potential window (Figure 1-c), simultaneously with the appearance of the second plateau at low potential, corresponding to an increase of the reversible capacity to 650 mAh g^{-1}. In such conditions a good capacity retention is maintained up to the 160th cycle. The two plateaux were

explained by a two clearly distinct step reversible conversion and alloying reactions.[13]

As mentioned in the introduction, the cycling of these two electrodes was deemed satisfactory based on these preliminary results in sodium half-cells. It is noteworthy that these two electrodes show much better cycling performance in Na cells than in Li cells.[14, 15] The next part is dedicated to their performance in full cell as negative electrode vs $Na_x[Ni/Mn/Mg/Ti]O_2$ as positive electrode.

Full cell electrochemistry

For NIB full cell testing the Sn and SnSb negative electrodes were combined with positive electrodes based on a layered oxide positive electrode material supplied by Faradion. All cell testing was conducted at 30 °C. To limit the number of experimental variables the full cells were all tested under equivalent experimental conditions. The cell voltage limits for the charge discharge tests (CC/CV charge) were 1.0-4.2 V and the charge/discharge rates were approximately C/7.

Cell#	Negative electrode Material	Active Negative electrode / mg	Positive electrode Material	Positive electrode Active / mg	P:N Mass Ratio	Positive electrode mAh g^{-1} Cycle#1	Positive electrode mAh g^{-1} Cycle#50	Capacity fade %/cycle
A11016	Sb	6.4	Faradion	25.2	3.9	149.4	136.2	0.18
A12001	Sb	3.3	Faradion	16.8	5.1	147.3	132.2	0.21
A12005	Sb	3.55	Faradion	25.1	7.1	121.7	93.1	0.47
A11019	Sb	5.3	Faradion	15.6	2.94	145.2	128.4	0.23

Table 1. 3-Electrode Na-ion pouch cells incorporating Sb electrodes – using varying positive to negative (P:N) active mass balances.

Cell#	Negative electrode Material	Negative electrode Active / mg	Positive electrode Material	Positive electrode Active / mg	P:N Mass Ratio	Positive electrode mAh g^{-1} Cycle#1	Positive electrode mAh g^{-1} Cycle#50	Capacity fade %/cycle
A11010	SnSb	5.6	Faradion	21.4	3.8	137.7	135.3	0.04
A12021	SnSb	5	Faradion	25.9	5.2	125.0	118.3	0.11
A12023	SnSb	5.3	Faradion	31.7	6.0	132.4	118.3	0.15
A11028	SnSb	3.3	Faradion	15.3	4.6	130.4	127.8	0.05
A11029	SnSb	5.2	Faradion	34.5	6.6	133.6	116.6	0.25

Table 2. 3-Electrode Na-ion pouch cells incorporating SnSb electrodes – using varying positive to negative (P:N) active mass balances.

3E Full-cell Electrochemistry

Sb as negative electrode:

To evaluate the electrochemical performance of the Sb and SnSb active materials in a realistic pre-commercial environment, 3-electrode Na-ion pouch cells with different mass balance were built as detailed in the Tables 1 and 2 respectively. In this configuration the Faradion positive electrode material was employed while a piece of sodium metal pressed onto aluminium tab was used as a reference-electrode (RE). The 3-electrode cells allow us to monitor and elucidate the full cell voltage response and the individual electrode potential

responses as a function of the active material utilization. The negative to positive active mass ratio was varied in these iterations since we expected some of the key battery performance indicators (for example, capacity fade during cycling, operating voltage etc.) to be determined and controlled by the negative electrode reversible specific capacity.

The data from these cells are presented in the following figures and in all cases the voltage profiles of the second cycle are shown. For each iteration the figures show the cell voltage response (in V) and the individual electrode potential response (in V vs. Na reference) as a function of the cumulative active specific capacity. To limit the number of variables, the cell voltage limits and the constant current rates for charge and discharge were kept constant in all i tively.

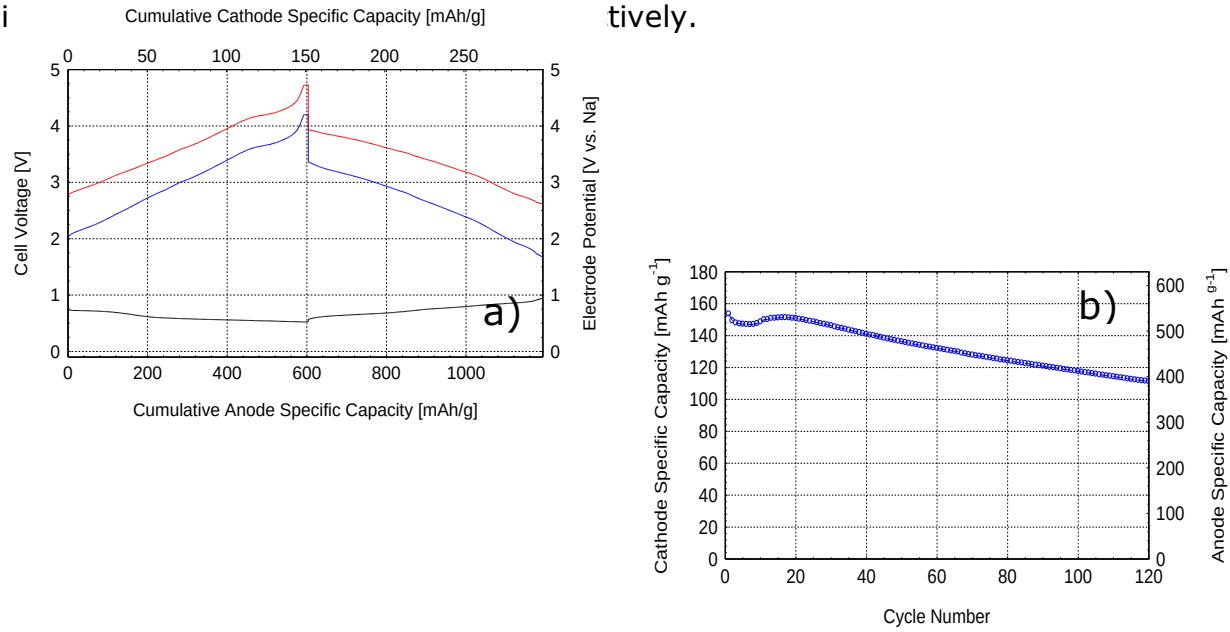

***Figure 2 a and b**: Cell#A11016 3E Cell - 2nd cycle. Sb electrode matched with Faradion Positive electrode; Positive to negative active mass balance = 3.9:1. Left. Blue: Cell Voltage Response (V), Red: Positive Electrode Potential (V vs. Na), Black: Negative Electrode Potential (V vs. Na). Reversible positive electrode specific capacity = 149* mAh g^{-1}*; Reversible negative electrode specific capacity*

= 589 mAh g^{-1}*. Average discharge cell voltage = 2.61 V. Right. Lifetime cycling using cell voltage limits of 1.0 - 4.2 V and ±C/7.*

The electrochemical performance of Cell#A11016 is depicted in Figure 2. In this particular configuration, the electrode mass ratio was 3.9 (i.e. P/N ratio, 3.9:1). The electrode potential responses indicate clearly that the Na-ion cell is capacity imbalanced. The negative electrode response reaches only around 0.5 V vs. Na when the cell is fully charged (cell voltage = 4.2 V). The pinning of the negative electrode at this relatively high potential forces the positive electrode potential into a state of relative over-charge – around 4.7 V vs. Na at the end of the cell charging process.

Encouragingly, this extremely oxidative potential allows an increased cathode material utilization – indeed the positive active material delivers a reversible specific capacity of over 149 mAh g^{-1}. This corresponds to a negative active material utilization of 589 mAh g^{-1} (i.e. 89% of the theoretical capacity). Considering these extreme testing conditions, rather counter-intuitively the cell demonstrates a low-capacity fade rate of 0.18%/cycle over the first 50 cycles (see Figure 2b). It is also worth noting that the capacity declines during the first 10 cycles before it increases up to the 20^{th} cycle and then slowly decreases in the subsequent 100 cycles. The capacity increase in the first 20 cycles may be explained by improved wettability of the electrodes with electrolyte over time, leading to the higher utilisation of the electrodes.

A closer inspection of the data collected for this cell indicates that the voltage profile of the negative electrode for the second cycle (sodiation) up to a capacity

of 400 mAh g^{-1} is similar to the voltage profile data recorded from the half-cell (Figure 2a). The half-cell is slightly more polarised, likely caused by the sodium metal counter electrode which may be covered by decomposition reaction products arising from the reaction between the electrolyte and the sodium metal. In the case of the 3-electrode cell, the absence of any additional features at cell voltage lower than 0.5 V may be explained by the lower polarisation of the negative electrode and the cut-off voltage of 4.2 V. Indeed, as has been noted, when the cell voltage reached a voltage of 4.2 V, the voltage of the positive electrode was 4.7 V vs. Na and the negative electrode voltage was 0.5 V vs. Na.

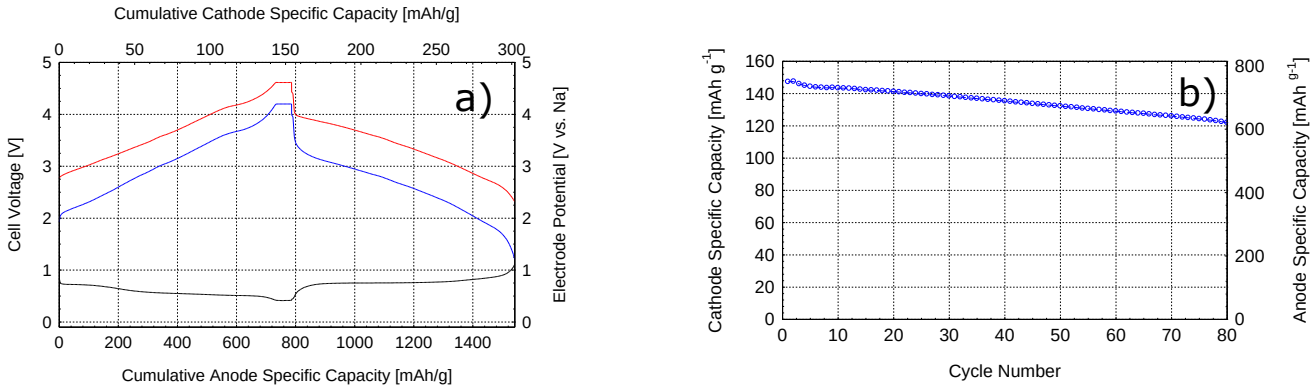

***Figure 3 a and b**: Cell#A12001 3E Cell2nd cycle. Sb electrode matched with Faradion Positive electrode; Positive to negative active mass balance = 5.1:1. Left. Blue: Cell Voltage Response (V), Red: Positive Electrode Potential (V vs. Na), Black: Negative Electrode Potential (V vs. Na). Reversible positive electrode specific capacity = 147.3* mAh g^{-1}*; Reversible negative electrode specific capacity = 750.0* mAh g^{-1}*. Average discharge cell voltage = 2.58 V. Right. Lifetime cycling using cell voltage limits of 1.0 - 4.2 V and ±C/7.*

In Figure 3 we demonstrate the effect on cell performance on moving to a higher positive/negative cell balance (P/N ratio, 5.1:1). As expected, under this experimental condition we determine a corresponding increase in the negative electrode reversible specific capacity. In addition, we detect that the negative voltage response also shows a move away from the first Na insertion plateau. This limits the upper potential of the positive electrode at the end of the cell charge and we would consider the cell to be in an improved electrode capacity balance. Similarly, to cell#A11016 (Figure 2a) the positive active material demonstrates excellent reversible utilization – around 147 mAh g^{-1}. The full cell lifetime cycling is also encouraging. We demonstrate a capacity fade rate of 0.21%/cycle for the first 50 cycles (see Figure 3 b). Surprisingly, the discharge capacities of first cycles for Sb electrode are greater than the theoretical capacity of 660 mAh g^{-1}. It could arise from SEI that is massively formed during the first cycles as a result of volume changes of 390 % during the alloying and dealloying reactions in which fresh reactive surfaces could be formed. A second explanation could be the uncertainty coming from the both not calendered Sb and not optimized laboratory's electrodes, presenting obvious inhomogeneity in the active material (Sb) dispersion. The loss of capacity appears more rapid during the 5 first cycles, which could (as explained above) be attributed to the SEI formation on the negative electrode, which contributes to irreversibly trapped Na^+ (i.e. loss of Na inventory), especially during the first cycles.[16]

The highest P/N cell balance (in this case, P/N ratio, 7.1:1) for the Sb material was tested in Cell#A12005. In this case we see clear evidence for Na plating on charge, denoted by the negative electrode reaching 0 V vs. Na reference (see the negative voltage response in Figure SI-2 a). This was confirmed by visual

inspection of the Sb electrode, harvested upon cell dismantling following the lifetime cycling regime, where clear evidence for plating was noted on the surface of the Sb. The Na plating process at the negative electrode pins the positive electrode potential at 4.2 V vs. Na on full cell charge. This limits the positive active specific capacity performance at about 122 mAh g^{-1}. In this condition the higher amount of positive electrode (Na source) counteracts both effects of the unavoidable Na trapping in the SEI on the negative electrode and the Na plating, which results in a stable capacity during the three first cycles. Thereafter the rate of capacity fade increases, presumably as a direct consequence of the extensive Na plating (Figure SI-2 b). We demonstrate a capacity fade rate of 0.47%/cycle for the first 50 cycles.

To further evaluate the commercial relevance of the Sb material we investigated the cycle life performance of the full Na-ion cells. Figure 4 depicts the specific capacity fade behaviour for both anode and cathode as a function of cycle number for the different P/N ratios. With varying P/N ratios from 2.9 to 7.1, the positive electrode 1^{st} cycle capacity was in the range of 120-150 mAh g^{-1} while the negative electrode capacity was between 400-870 mAh g^{-1}. P/N ratios of 2.9, 3.9 and 5.1 show reasonable capacity retention, while P/N of 7.1 shows much rapid capacity fade. The sudden capacity of decay of cell A12001 (P/N ratio of 5.1) at cycle 75 could be caused by a sudden increase of the cell impedance. The gradual capacity fading with increasing cycle number is probably caused by the formation of newly fresh active Sb surfaces which are created from the drastic volume changes and which will be passivated when in contact with the electrolyte. The passivation layer thickens up upon cycling and impedes sodium ion transport. Furthermore, as the result of the huge volume expansion, the electrical disconnection between active particles is likely to occur. These two

combined phenomena which occur over time are probably the causes of the cell failure. Limiting the electrochemical window for such negative electrodes, would decrease volume changes and mitigate the onset of cell failure. Moreover, further tests of calendering of electrodes, which is a very important parameter especially for negative electrode, are planned and would optimize the capacity retention, the reproducibility and avoid this kind of sudden capacity decay.

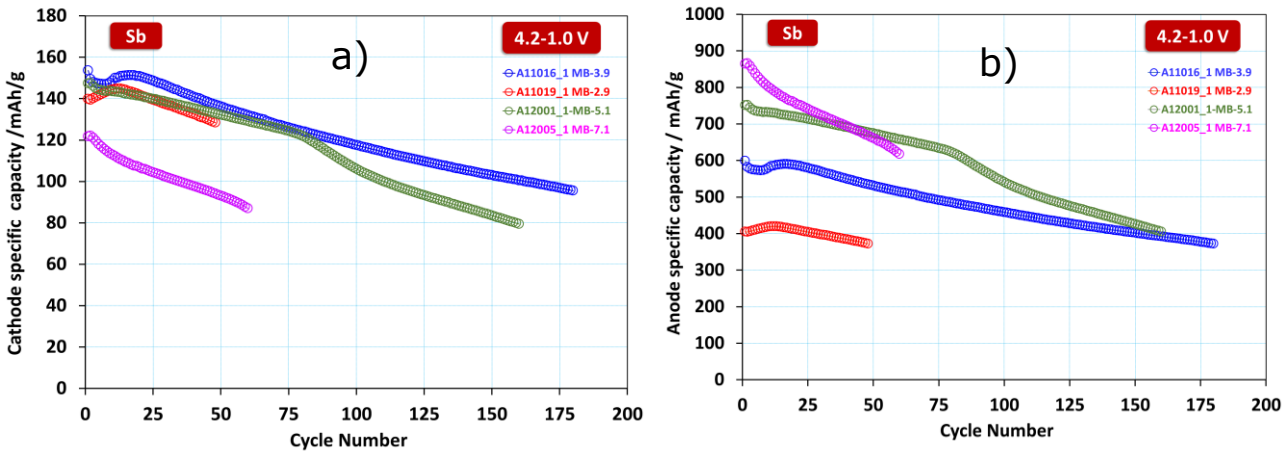

***Figure 4**:* the specific capacity retention a) of the positive electrode and b) of the negative electrode for the different P/N ratios.

Unsurprisingly, the higher P/N ratio increases the capacity of the negative electrode while the capacity of the positive electrode remains fairly constant with the exception of P/N ratio of 7.1. In this case the amount of Na supplied by the positive electrode is excessive and results immediately in the plating of sodium plated on the negative electrode, and/or consumed in the SEI formation, leading to a relatively poor capacity retention.

Encouragingly for the cell at P/N of 5.1, though the specific capacity of the negative electrode is very high the cycle life is reasonably good, despite the risk of Na plating, SEI formation and high-volume material expansion.

The best capacity retention was obtained with the mass balance of 3.9, which still delivers a capacity of 97 mAh g^{-1} for the positive electrode after 180 cycles and 380 mAh g^{-1} for the negative electrode. The cell with P/N ratio of 2.9 delivers a too low amount of Na^+ to get a full use of the Sb electrode. The starting capacity is only around 400 mAh g^{-1}, and the capacity loss is relatively low.

From a commercial perspective, the data presented here suggest that further optimisation of the Sb negative electrode will be required along with the use of an improved electrolyte system.

SnSb as negative electrode:

The similar experimental approach was applied to optimize the P/N balancing of the SnSb as negative (N) electrodes. In that case, as shown Figure 1-c for the cycling in half cell, two voltage plateaus occur at low potential (0.5 and 0.01V vs. Na).

The second cycle performance data for 3E Cell#A11010 is shown in Figure 5. Based on the electrode potential responses (Figure 5 a), the cell appears to be reasonably well-balanced. Note the negative electrode and positive electrode potentials at full cell on charge. Under these circumstances the Na-ion cell is well balanced and cycling quite well. The P/N ratio of 3.8 allows the SnSb negative electrode material to deliver a reversible specific capacity of around 532 mAh g^{-1} and reach around 0.15 V vs. Na on full cell charge, which represents however only 71% of the theoretical capacity in agreement with the absence of the 0.01V plateau.

This material utilization for the SnSb electrode is nevertheless around double that recorded for a commercial hard carbon.[1-3] This pins the positive electrode at 4.35 V vs. Na on full cell charge and allows the active material to deliver a reversible specific capacity of about 139 mAh g^{-1}.

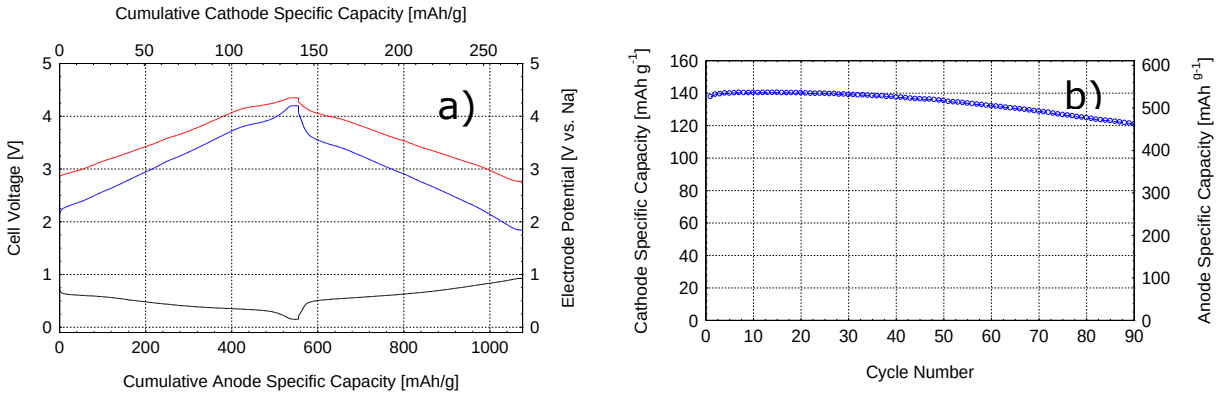

***Figure 5 a and b**: Cell#A11010 3E Cell - 2nd cycle. SnSb electrode matched with Faradion Positive electrode; Positive to negative active mass balance = 3.8:1. Left. Blue: Cell Voltage Response (V), Red: Positive Electrode Potential (V vs. Na), Black: Negative Electrode Potential (V vs. Na). Reversible positive electrode specific capacity = 139.3* mAh g^{-1}*; Reversible negative electrode specific capacity = 532.3* mAh g^{-1}*. Average discharge cell voltage = 2.61 V. Right. Lifetime cycling using cell voltage limits of 1.0 - 4.2 V and ±C/7.*

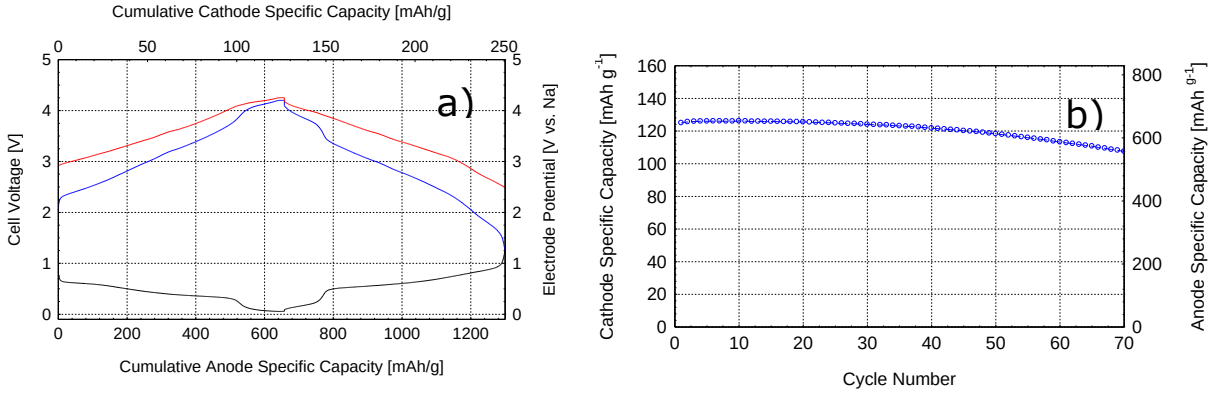

***Figure 6 a and b**: Cell#A12021 3E Cell - 2nd cycle. SnSb electrode matched with Faradion Positive electrode; Positive to negative active mass balance = 5.2:1. Left. Blue: Cell Voltage Response (V), Red: Positive Electrode Potential (V vs. Na), Black: Negative Electrode Potential (V vs. Na). Reversible positive electrode specific capacity = 125.0* mAh g^{-1}*; Reversible negative electrode specific capacity = 647.5* mAh g^{-1}. *Average discharge cell voltage = 2.84 V. Right. Lifetime cycling using cell voltage limits of 1.0 - 4.2 V and ±C/7.*

The cycling data in Figure 5 b confirm the excellent reversibility for this cell combined to very low fading for the first 90 full depth-of-discharge cycles. We demonstrate a capacity fade rate of just 0.04%/cycle for the first 50 cycles. This is very encouraging cycling performance.

In Cell#A12021 we assess the effect of increasing the P/N cell balance to 5.2 (Figure 6 a). The sodiation mechanism for the SnSb negative electrode materials enters the second plateau with at full cell charge a potential to +30 mV from Na metal potential. Then it delivers a higher capacity of 648 mAh g^{-1} which represents 86% of the theoretical capacity, when the positive material operates at about 125 mAh g^{-1}. The electrode potentials are comfortably within the stable electrochemical stability window for the electrolyte. The cycling data in Figure 6 b confirm the excellent reversibility for this cell combined to very low capacity fade behaviour for the first 90 full depth-of-discharge cycles. We demonstrate a capacity fade rate of 0.11%/cycle for the first 50 cycles. Dismantling of the cell following the lifetime cycling regime confirmed (by visual inspection) that no Na plating had taken place on the negative electrode.

The effects of further increasing the P/N balance (in this case to 6:1) is shown for Cell#A12023 in Figure SI-4. The increased cell balance has the effect of

improving the reversible capacity of the SnSb active material. The voltage response for the negative electrode again clearly demonstrates the dual-plateau sodiation mechanism. At full cell charge the negative electrode potential is about +20 mV from Na metal potential. The negative active material delivers around 792 mAh g^{-1} (slightly higher than the theoretical capacity 752 mAh g^{-1}) while the positive material operates at about 132 mAh g^{-1}.

As was observed for Cell#A12021, the electrode potentials are comfortably within the stable electrochemical stability window for the electrolyte, so we should expect reasonably good cycling performance with relatively low-capacity fade.

A further increase in the P/N cell balance (i.e. P/N ratio, 6.6) clearly demonstrates the dual-plateau sodiation mechanism for the negative electrode material (Cell#A11029, Figure SI-5). At full cell charge the negative electrode potential is about +20 mV from Na metal potential, corresponding to a comfortable stable electrochemical stability window (no Na plating). The negative active material delivers around 792 mAh g^{-1} while the positive material operates at about 132 mAh g^{-1}. The cycling data (Figure SI-5 b) confirm th

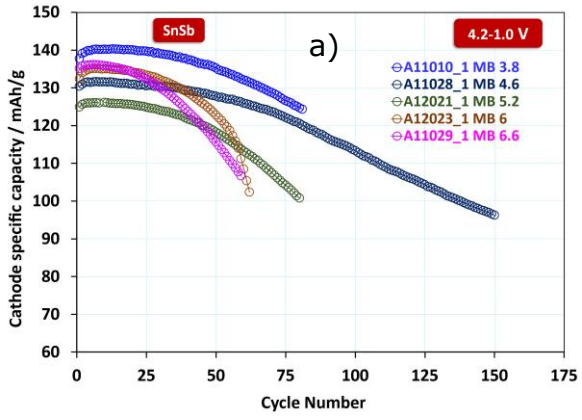

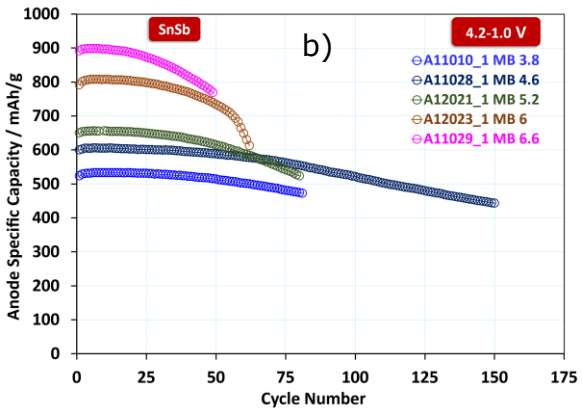

***Figure 7**: the specific capacity retention a) of the positive electrode and b) of the SnSb for the different P/N ratios cells.*

excellent reversibility for this cell combined to very low capacity fade behaviour for the first 60 full depth-of-discharge cycles.The capacity fade behaviour as a function of cycle number of both electrodes is illustrated in Figure 7 for five different P/N ratios. With varying P/N ratios of 3.8-6.0, for the first cycles positive electrode capacity is between 125-140 mAh g^{-1} while for the negative electrode a capacity between 500-900 mAh g^{-1} is measured. Unsurprisingly as for Sb electrode, higher P/N ratio increases the utilisation of the negative electrode capacity and its capacity while the capacity of the positive electrode remains in the range of 125-140 mAh g^{-1}. The lower P/N ratios, 3.8, 4.6 and 5.2, show excellent capacity retention for the first 50 cycles with the capacity retention of 98, 98 and 95% of the 1^{st} cycle capacity. The P/N ratio of 4.6 maintains 75% of the 1^{st} cycle capacity after 150 cycles.

For P/N ratios of 6.0 and 6.6 the amount of Na^+ supplied by the positive electrode is excessive, but surprisingly no plating was found on the negative electrode. The cycling at very low potential increases however the extent of SEI formation, which after few cycles increases the resistivity of the negative electrode and hampers its satisfactory operation. The cycling of the negative electrode at capacity higher than 800 mAh g^{-1} results of a whole alloying process (SnSb into Na_3Sb and $Na_{15}Sn_4$) and a maximum volume expansion of the electrode leading to electrical disconnection of the active material from the carbon conductive additives and possibly electrode cracking and pulverisation. New surfaces will be formed that will be passivated. Furthermore, it is likely that

the SEI will break down and reform. All these parasitic reactions are likely to increase the resistance of the negative electrode and will hamper the cyclability of the cell.

It is noticeable that the Sb/Na half-cell cycling (Figure 1) appeared more stable than that of SnSb/Na half-cell while capacity retention in full cell appears slightly better for SnSb than for Sb (Figure 4 and 7).

One explanation could be that SnSb reacts vs Na in two main potential plateaus. The second one is at very low potential, meaning a huge SEI formation occurs, while it is a bit limited by the higher sodiation potential for Sb/Na. In full cell, as the Na content is limited by the cathode amount, the SEI formation on the negative electrode is limited, in consequence lower resistive layer is accumulated and the situation becomes better for the SnSb/Na cell.

2E Full-cell Electrochemistry, cycling, rate

Figure 8 presents the specific capacity and capacity retention normalised to the capacity obtained at C/5 for the P/N ratio of 3.44 at different discharge rates from C/5 to 2C. A new lower P/N ratio was chosen so as to minimise the volume changes and limit the capacity of the anode. The capacity retention at different rates is shown on the graph. At C/5 rate, the positive electrode delivered a specific capacity of 145 mAh g^{-1} and the negative electrode delivered a capacity of 500 mAh g^{-1}. As the rate increases to 2C, the capacity decreases to 119 mAh g^{-1} for the positive electrode and 412 mAh g^{-1} for the negative electrode, which corresponds to 82% of the capacity measured at C/5.

Figure SI-6 shows the cycle life of the cell cycling at a charge/discharge rate of C/5, after the series of cycles at higher rates (Figure 8). Good cycle life was

obtained with a capacity retention of 80% after 100 cycles corresponding to a negative electrode capacity up to 400 mAh g^{-1}.

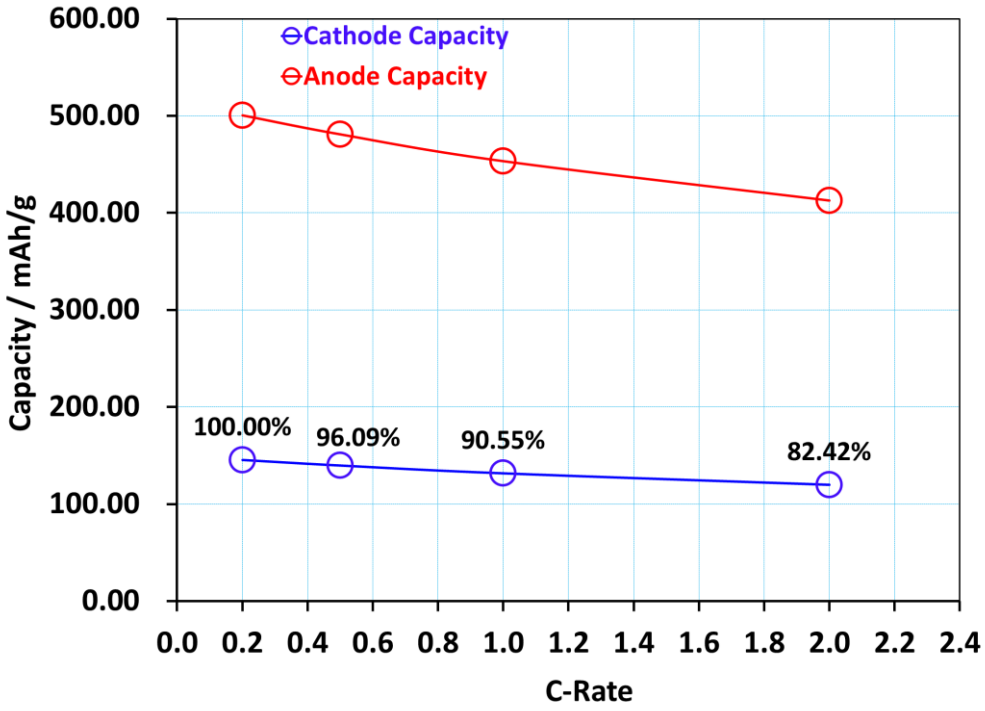

***Figure 8**:* the specific capacity retention for the P/N ratio of 3.44 of both electrodes at different rates from C/5 to 2C.

Even the system would be further optimised by working on both the negative electrode formulation and a judicious choice of electrolyte, these preliminary tests of P/SnSb full cells are extremely encouraging in terms of cycle life as well as rate capability.

4. Discussions

This evaluation of Na-ion full cells involving the Sb and SnSb materials as negative electrodes demonstrates the important role of the P/N ratio in the cycling performance, which is not easy to predict.

For both systems, too low a P/N ratio leads to overcharge of the positive electrode, while too high a mass balance leads to Na plating. For both negative electrodes, satisfactory cycling (i.e. low capacity fade over an extended cycling regime range) was achieved at a fairly wide range of P/N cell balances, from 4.5 to 5.5 and 5.0 to 6.0 for cell incorporating Sb and SnSb, respectively. Under these experimental conditions no Na plating was observed confirming that the higher average operating voltage (V vs. Na) of the alloy electrodes (Sb, SnSb) is an advantage compared to HC to prevent Na plating.

The rate performance of cells incorporating SnSb is encouraging with the delivered capacity only slightly affected by the increase to the highest discharge rate (2C). This benefit is likely derived from the use of relatively thin electrodes allowing high negative electrode capacity, showing lower impedance and finally higher rate capability. These systems could be useful for fast charge acceptance, which represent a challenge for the future batteries generations.

Even though the Na-ion cells incorporating Sb and SnSb require further optimization, it appears interesting to do an initial, rough estimation of the energy which could be delivered by a prototype pouch cell. We have modelled and estimated the capacity and energy density of a pouch cell of dimension 180 mm wide, 213 mm long and 10 mm thick. In this model, we have used the data shown in figure 8, cathode capacity of 145 mAh g^{-1} and anode capacity of 500 mAh g^{-1} and a P/N ratio of 3.4. Taking into consideration of the higher density of SnSb 6.9 g/cm3 over hard carbon 1.4 g/cm^3 for hard carbon, a cell capacity of 49 Ah with an energy density of 183 Wh/kg were estimated.

This first estimation is encouraging if we compare with the previously quoted cell specific energy of 150-160 W h kg^{-1} of Faradion cells based on Ni based positive electrode and HC.[17] Of course, the negative electrode studied herein is not directly comparable to the already widely produced HC, which is the common sodium battery negative electrode material and is manufactured in commercial volumes.

On the other hand, these results are encouraging if we consider the rare studies presenting antimony based full cells performance. For example, Cheng et al studied a full Na-ion cell with Sb/rGO and $Na_3V_2(PO_4)_3$/rGO as negative and positive electrode, respectively, delivering a reversible capacity of ≈ 400 mAh g^{-1} (for the negative) after 100 cycles.[18]

5. Conclusions

Na-ion batteries (SIB) represent a realistic and important alternative to commercial Li-ion batteries. Due to the availability of Na precursor, its lower cost and improved safety characteristics SIB are expected to play a future role in the future stationary electrochemical systems and also for the E-mobility.

The search for next-generation negative electrode active materials for Na-ion is critically important, especially to replace hard carbon. To challenge the LIB, these new negative electrodes have to compete with Si/graphite composite electrodes. Briefly for commercial applications the active materials must be: low-cost, high reversible specific capacity, good cyclability, low voltage vs. Na, and lower voltage hysteresis etc.

As Na-metal Sb and SnSb half-cells have shown very encouraging performance, much better than vs Li, their study in full cells appeared obvious. We chose a Faradion positive electrode, a mixed phase O3/P2 layered oxide as positive electrode, which works very well under all experimental conditions. By working on the P/N balance, we demonstrated that the full cell Na-ion cell data are good even at non-optimized cell balances. No Na plating is evident unless working at very high positive/negative cell balance. The higher average operating voltage (vs. Na) of the alloy electrodes when compared to HC makes it is easier to prevent Na plating in the full Na-ion cells. Rather counter-intuitively, it is not always the cell using the apparently 'optimized' cell balance that demonstrates the lowest capacity fade behaviour during cycling. High cyclability can be achieved at a fairly wide range of cell balances.

Rate performance is encouraging and likely a consequence using relatively thin negative electrodes due to the high specific capacity of the Sb and SnSb active materials. Note it should also help the cell's power capability, which could be a real advantage for applications required fast charge acceptance.

Acknowledgment :

The authors would like to thank Faradion Limited for permission to publish this work. LM and JF would like to thank colleagues from RS2E (the French National Research Agency (STORE-EX Labex Project ANR-10-LABX-76-01) for fruitful discussions.

Declaration of competing interest

The authors declare that they have no known competing financial interests or personal relationships that could have appeared to influence the work reported in this paper.

References

[1] R. Alcantara, J.M. Jimenez-Mateos, P. Lavela, J.L. Tirado, Carbon black: a promising electrode material for sodium-ion batteries, Electrochem Commun.;3(11) (2001) 639

[2] D.A. Stevens, J.R. Dahn, High capacity anode materials for rechargeable sodium-ion batteries, J Electrochem Soc., 147(4), (2000) 1271

[3] S. Komaba, W. Murata, T. Ishikawa, N. Yabuuchi, T. Ozeki, T. Nakayama, A. Ogata, K. Gotoh, K. Fujiwara, Electrochemical Na Insertion and Solid Electrolyte Interphase for Hard-Carbon Electrodes and Application to Na-Ion Batteries, Adv Funct Mater., 21(20), (2011) 3859

[4] Chapter 5, Na-ion batteries; L. Monconduit, L. Croguennec, Eds.; ISTE & John Wiley and Sons: London, New York, 2021 ISBN 9781789450132

[5] V.L. Chevrier, G. Ceder, Challenges for Na-ion Negative Electrodes. Journal of The Electrochemical Society, 158(9), (2011) A1011

[6] J. Qian; Y. Chen, L. Wu, Y. Cao, X. Ai, H. Yang, High capacity Na-storage and superior cyclability of nanocomposite Sb/C anode for Na-ion batteries, Chem. Commun. 48 (2012) 7070.

[7] A. Darwiche, C. Marino, M. T. Sougrati, B. Fraisse, L. Stievano, L. Monconduit, Better cycling performances of bulk Sb in Na-ion batteries compared to Li-ion systems: an unexpected electrochemical mechanism J. Am. Chem. Soc., 134 (51), (2012) 20805–20811

[8] P. K. Allan, J. M. Griffin, A. Darwiche, O. J. Borkiewicz, K. M. Wiaderek, K. W. Chapman, P. J. Chupas, L. Monconduit, C. P. Grey, Tracking sodium-antimonide phase transformations in sodium-ion anodes; insights from in operando pair distribution function analysis and solid-state NMR, J. Am. Chem. Soc., 138, (2016) 2352−2365

[9] L. Wu, X.H. Hu, J.F. Qian, F. Pei, F.Y. Wu, R.J. Mao, X.P. Ai, H.X. Yang, Y.L. Cao, Sb–C nanofibers with long cycle life as an anode material for high-performance sodium-ion batteries. Energy Environ. Sci. 7 (2014) 323-328.

[10] K. Yang, J. Tang, Y. Liu, M. Kong, B. Zhou, Y. Shang, W.H. Zhang, Controllable Synthesis of Peapod-like Sb@C and Corn-like C@Sb Nanotubes for Sodium Storage. ACS Nano 14 (2020) 5728-5737.

[11] A.Darwiche, M. T. Sougrati, B. Fraisse, L. Stievano, L. Monconduit, Facile synthesis and long cycle life of SnSb as negative electrode material for Na-ion batteries Electrochem.Comm., 201 (2013) 18–21

[12] J. Barker and R. Heap, O3/P2 mixed phase sodium-containing doped layered oxide materials. WO Application 2019197812, in, Faradion Limited (2020

(priority date April 9, 2018)).
R. Sayers, J. Barker and R. Heap, Compositions containing doped nickelate compounds. US Patent 10550007, in (2020 (priority date May 22, 2014)).

[13] M. Fehse, M. T. Sougrati, A. Darwiche, V. Gabaudan, C. La Fontaine, L. Monconduit, L. Stievano, Elucidating the origin of superior electrochemical cycling performance: new insights on sodiation–desodiation mechanism of SnSb from operando spectroscopy, J. Mater. Chem. A, 6 (2018) 8724-8734

[14] P. Antitomaso, B. Fraisse, L. Stievano, S. Biscaglia, D. Aymé-Perrot, P. Girard, M. T. Sougrati, L. Monconduit, SnSb electrode for Li-ion batteries: electrochemical mechanism and capacity fading origins elucidated by Operando techniques Journal of Materials, Chemistry A (2017) 5, 6546-6555
[15] F. J. Fernandez-Madrigal, et al., X-ray Diffraction, 7Li MAS NMR spectroscopy, and 119 Sn m¨ossbauer spectroscopy study of SnSb-based electrode materials, Chem. Mater., 2002, 14, 2962–2968
[16] A. Darwiche, L. Bodenes, L. Madec, L. Monconduit, H. Martinez, Impact of the salts and solvents on the SEI formation in Sb/Na batteries: An XPS analysis, Electrochimica Acta, 207, 20 (2016) 284–292

[17] A. Bauer, J. Song, S. Vail, W. Pan, J. Barker, Y. Lu, The Scale-up and Commercialization of Nonaqueous Na-Ion Battery Technologies, Adv. Energy. Mater, 8 (2018) 1702869

[18] De-Liang Cheng, L. Yang, M. Zhu, High-performance anode materials for Na-ion batteries, Rare Metals 37(2018)167–180